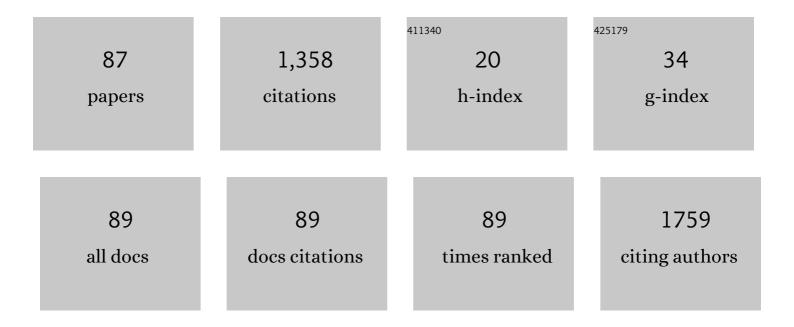
## Philippe C Després

List of Publications by Year in descending order

Source: https://exaly.com/author-pdf/4389341/publications.pdf Version: 2024-02-01



#	Article	IF	CITATIONS
1	Beam-hardening corrections through a polychromatic projection model integrated to an iterative reconstruction algorithm. NDT and E International, 2022, 126, 102594.	1.7	3
2	Personalized Risk Assessment for Prevention and Early Detection of Breast Cancer: Integration and Implementation (PERSPECTIVE I&I). Journal of Personalized Medicine, 2021, 11, 511.	1.1	59
3	Exploring polypharmacy with artificial intelligence: data analysis protocol. BMC Medical Informatics and Decision Making, 2021, 21, 219.	1.5	4
4	Quantitative SPECT (QSPECT) at high count rates with contemporary SPECT/CT systems. EJNMMI Physics, 2021, 8, 73.	1.3	2
5	Identification of Common Minerals Using Stoichiometric Calibration Method for Dualâ€Energy CT. Geochemistry, Geophysics, Geosystems, 2021, 22, e2021GC009885.	1.0	7
6	Evaluating the impact of real-time multicriteria optimizers integrated with interactive plan navigation tools for HDR brachytherapy. Brachytherapy, 2020, 19, 607-617.	0.2	10
7	Validation of irtGPUMCD, a GPU-based Monte Carlo internal dosimetry framework for radionuclide therapy. Physica Medica, 2020, 73, 95-104.	0.4	5
8	Impact of dead time on quantitative 177Lu-SPECT (QSPECT) and kidney dosimetry during PRRT. EJNMMI Physics, 2020, 7, 32.	1.3	11
9	Dose to the bladder neck is not correlated with urinary toxicity in patients with prostate cancer treated with HDR brachytherapy boost. Brachytherapy, 2020, 19, 584-588.	0.2	2
10	DNA repair gene polymorphisms, tumor control, and treatment toxicity in prostate cancer patients treated with permanent implant prostate brachytherapy. Prostate, 2020, 80, 632-639.	1.2	3
11	Potential of iterative reconstruction for maxillofacial cone beam CT imaging: technical note. Neuroradiology, 2020, 62, 1511-1514.	1.1	3
12	Comprehensive SPECT/CT system characterization and calibration for 177Lu quantitative SPECT (QSPECT) with dead-time correction. EJNMMI Physics, 2020, 7, 10.	1.3	18
13	A Phase 2 Randomized Pilot Study Comparing High-Dose-Rate Brachytherapy and Low-Dose-Rate Brachytherapy as Monotherapy in Localized Prostate Cancer. Advances in Radiation Oncology, 2019, 4, 631-640.	0.6	21
14	Iterative reconstruction for image enhancement and dose reduction in diagnostic cone beam CT imaging. Journal of X-Ray Science and Technology, 2019, 27, 805-819.	0.7	5
15	<tt>pGPUMCD</tt> : an efficient GPU-based Monte Carlo code for accurate proton dose calculations. Physics in Medicine and Biology, 2019, 64, 085018.	1.6	6
16	A GPU-based multi-criteria optimization algorithm for HDR brachytherapy. Physics in Medicine and Biology, 2019, 64, 105005.	1.6	25
17	Does Seed Migration Increase the Risk of Second Malignancies in Prostate Cancer Patients Treated With Iodine-125 Loose Seeds Brachytherapy?. International Journal of Radiation Oncology Biology Physics, 2018, 100, 1190-1194.	0.4	5
18	A fast 4D cone beam CT reconstruction method based on the OSC-TV algorithm. Journal of X-Ray Science and Technology, 2018, 26, 189-208.	0.7	2

PHILIPPE C DESPRéS

#	Article	IF	CITATIONS
19	Efficiency improvement in proton dose calculations with an equivalent restricted stopping power formalism. Physics in Medicine and Biology, 2018, 63, 015019.	1.6	2
20	<scp>COMP</scp> report: <scp>CPQR</scp> technical quality control guidelines for <scp>CT</scp> simulators. Journal of Applied Clinical Medical Physics, 2018, 19, 12-17.	0.8	9
21	System matrix computation vs storage on GPU: A comparative study in cone beam CT. Medical Physics, 2018, 45, 579-588.	1.6	4
22	A multi-criteria optimization approach for HDR prostate brachytherapy: I. Pareto surface approximation. Physics in Medicine and Biology, 2018, 63, 205004.	1.6	9
23	A multi-criteria optimization approach for HDR prostate brachytherapy: II. Benchmark against clinical plans. Physics in Medicine and Biology, 2018, 63, 205005.	1.6	8
24	Multicenter Evaluation of Biochemical Relapse–Free Survival Outcomes for Intraoperatively Planned Prostate Brachytherapy Using an Automated Delivery System. International Journal of Radiation Oncology Biology Physics, 2017, 99, 895-903.	0.4	8
25	Conception and characterization of a virtual coplanar grid for a 11×11 pixelated CZT detector. Nuclear Instruments and Methods in Physics Research, Section A: Accelerators, Spectrometers, Detectors and Associated Equipment, 2017, 860, 62-69.	0.7	5
26	A review of GPU-based medical image reconstruction. Physica Medica, 2017, 42, 76-92.	0.4	57
27	High-dose-rate brachytherapy boost for prostate cancer treatment: Different combinations of hypofractionated regimens and clinical outcomes. Radiotherapy and Oncology, 2017, 124, 49-55.	0.3	31
28	A CZT-based blood counter for quantitative molecular imaging. EJNMMI Physics, 2017, 4, 18.	1.3	3
29	Validation of the French-Canadian version of the Expanded Prostate Cancer Index Composite (EPIC) in a French-Canadian population. Canadian Urological Association Journal, 2017, 11, 404-10.	0.3	10
30	Does prostate volume has an impact on biochemical failure in patients with localized prostate cancer treated with HDR boost?. Radiotherapy and Oncology, 2016, 121, 304-309.	0.3	5
31	CT dose reduction: approaches, strategies and results from a province-wide program in Quebec. Journal of Radiological Protection, 2016, 36, 346-362.	0.6	4
32	Image-guided high-dose-rate brachytherapy boost to the dominant intraprostatic lesion using multiparametric magnetic resonance imaging including spectroscopy: Results of a prospective study. Brachytherapy, 2016, 15, 746-751.	0.2	19
33	GPUâ€accelerated regularized iterative reconstruction for fewâ€view cone beam CT. Medical Physics, 2015, 42, 1505-1517.	1.6	39
34	Evaluation of the OSCâ€TV iterative reconstruction algorithm for coneâ€beam optical CT. Medical Physics, 2015, 42, 6376-6386.	1.6	12
35	A study of potential numerical pitfalls in GPU-based Monte Carlo dose calculation. Physics in Medicine and Biology, 2015, 60, 5007-5018.	1.6	9
36	GGEMS-Brachy: GPU GEant4-based Monte Carlo simulation for brachytherapy applications. Physics in Medicine and Biology, 2015, 60, 4987-5006.	1.6	18

PHILIPPE C DESPRéS

#	Article	IF	CITATIONS
37	Fast GPU-based Monte Carlo simulations for LDR prostate brachytherapy. Physics in Medicine and Biology, 2015, 60, 4973-4986.	1.6	15
38	Special section: Selected papers from the Fifth International Workshop on Monte Carlo Techniques in Medical Physics. Physics in Medicine and Biology, 2015, 60, 4947-4950.	1.6	0
39	Fast GPU-based computation of spatial multigrid multiframe LMEM for PET. Medical and Biological Engineering and Computing, 2015, 53, 791-803.	1.6	3
40	Sci-Thur AM: YIS - 03: irtGPUMCD: a new GPU-calculated dosimetry code for 177 Lu-octreotate radionuclide therapy of neuroendocrine tumors. Medical Physics, 2014, 41, 1-1.	1.6	1
41	Sci-Thur PM: Imaging - 05: Calibration of a SPECT/CT camera for quantitative SPECT with 99m Tc. Medical Physics, 2014, 41, 4-4.	1.6	0
42	Sci-Sat AM: Brachy - 07: Plastic scintillation detector validation for kV dosimetry. Medical Physics, 2012, 39, 4646-4646.	1.6	0
43	Sub-second high dose rate brachytherapy Monte Carlo dose calculations with <b><tt>bGPUMCD</tt></b> . Medical Physics, 2012, 39, 4559-4567.	1.6	20
44	Fast GPU-based computation of the sensitivity matrix for a PET list-mode OSEM algorithm. Physics in Medicine and Biology, 2012, 57, 6279-6293.	1.6	5
45	Validating plastic scintillation detectors for photon dosimetry in the radiologic energy range. Medical Physics, 2012, 39, 5308-5316.	1.6	45
46	The importance of an exponential prostate-specific antigen decline after external beam radiotherapy for intermediate risk prostate cancer. Cancer Epidemiology, 2012, 36, e137-e141.	0.8	3
47	Simultaneous Integrated Boost Using Intensity-Modulated Radiotherapy Compared With Conventional Radiotherapy in Patients Treated With Concurrent Carboplatin and 5-Fluorouracil for Locally Advanced Oropharyngeal Carcinoma. International Journal of Radiation Oncology Biology Physics, 2012. 82. 582-589.	0.4	44
48	The Role of Computed Tomography in the Management of the Neck After Chemoradiotherapy in Patients With Head-and-Neck Cancer. International Journal of Radiation Oncology Biology Physics, 2012, 82, 567-573.	0.4	42
49	Cervical Lymph Node Metastases From Unknown Primary Cancer: A Single-Institution Experience With Intensity-Modulated Radiotherapy. International Journal of Radiation Oncology Biology Physics, 2012, 82, 1866-1871.	0.4	24
50	Real-time processing in dynamic ultrasound elastography: A GPU-based implementation using CUDA. , 2012, , .		5
51	Special section: Selected papers from the Fourth International Workshop on Recent Advances in Monte Carlo Techniques for Radiation Therapy. Physics in Medicine and Biology, 2012, 57, .	1.6	3
52	TH-F-211-04: A Fast Finite Size Pencil Beam Algorithm for Dose Calculation Using GPUs. Medical Physics, 2012, 39, 4020-4021.	1.6	0
53	<scp>GPUMCD</scp> : A new GPUâ€oriented Monte Carlo dose calculation platform. Medical Physics, 2011, 38, 754-764.	1.6	181
54	18F-FDG-PET imaging in radiotherapy tumor volume delineation in treatment of head and neck cancer. Radiotherapy and Oncology, 2011, 101, 362-368.	0.3	56

PHILIPPE C DESPRéS

4

#	Article	IF	CITATIONS
55	Enteral Feeding During Chemoradiotherapy for Advanced Head-and-Neck Cancer: A Single-Institution Experience Using a Reactive Approach. International Journal of Radiation Oncology Biology Physics, 2011, 79, 763-769.	0.4	51
56	Fast dose calculation in magnetic fields with <tt>GPUMCD</tt> . Physics in Medicine and Biology, 2011, 56, 5119-5129.	1.6	92
57	Validation of GPUMCD for lowâ€energy brachytherapy seed dosimetry. Medical Physics, 2011, 38, 4101-4107.	1.6	16
58	TU-E-BRB-04: Fast Monte Carlo Calculations in Magnetic Fields with GPUMCD for the MRI-Linac. Medical Physics, 2011, 38, 3767-3767.	1.6	0
59	SU-E-I-172: Fast Computation of High Resolution LOR-Based 3D OSEM PET Algorithm Using the GPU Device. Medical Physics, 2011, 38, 3436-3436.	1.6	0
60	SU-E-T-683: Improvement of LDR Brachytherapy TG-43 Dose Calculations with a GPU-Accelerated Raytracing Algorithm. Medical Physics, 2011, 38, 3647-3647.	1.6	0
61	Concurrent Chemoradiation With Carboplatin–5-Fluorouracil Versus Cisplatin in Locally Advanced Oropharyngeal Cancers: Is More Always Better?. International Journal of Radiation Oncology Biology Physics, 2010, 76, 410-416.	0.4	22
62	A convolutionâ€superposition dose calculation engine for GPUs. Medical Physics, 2010, 37, 1029-1037.	1.6	33
63	Fast convolutionâ€superposition dose calculation on graphics hardware. Medical Physics, 2009, 36, 1998-2005.	1.6	49
64	SU-FF-T-622: Fast GPU-Based Raytracing Dose Calculations for Brachytherapy in Heterogeneous Media. Medical Physics, 2009, 36, 2668-2668.	1.6	1
65	TH-D-BRD-02: Convolution-Superposition Dose Calculations with GPUs. Medical Physics, 2009, 36, 2807-2807.	1.6	2
66	SU-FF-T-417: Effect of Transverse Magnetic Fields On MV Photon Dose Distributions in Heterogeneous Media. Medical Physics, 2009, 36, 2618-2618.	1.6	0
67	Stream processors: a new platform for Monte Carlo calculations. Journal of Physics: Conference Series, 2008, 102, 012007.	0.3	10
68	SU-GC-I-144: Validation of a Monte Carlo Model of the PET Component of the Gemini GXL PET/CT. Medical Physics, 2008, 35, 2675-2675.	1.6	0
69	TUâ€EEâ€A4â€06: Fast DRR and CBCT Reconstruction On GPU. Medical Physics, 2008, 35, 2915-2915.	1.6	1
70	Monte Carlo simulations of compact gamma cameras based on avalanche photodiodes. Physics in Medicine and Biology, 2007, 52, 3057-3074.	1.6	11
71	Evaluation of a MR-compatible CZT detector. , 2007, , .		3

FFT and cone-beam CT reconstruction on graphics hardware. , 2007, , .

5

Philippe C Després

#	Article	IF	CITATIONS
73	Joint registration of multiple images using entropic graphs. , 2007, , .		0
74	Modeling and Correction of Spatial Distortion in Position-Sensitive Avalanche Photodiodes. IEEE Transactions on Nuclear Science, 2007, 54, 23-29.	1.2	16
75	Investigation of a continuous crystal PSAPD-based gamma camera. IEEE Transactions on Nuclear Science, 2006, 53, 1643-1649.	1.2	14
76	Evaluation of a Large Pixellated Cadmium Zinc Telluride Detector for Small Animal Radionuclide Imaging. , 2006, , .		6
77	Reducing the Distortion in Resistive Layer Positioning Devices: A Simulation Study. , 2006, , .		0
78	Comparison of Position-Sensitive versus Discrete Avalanche Photodiodes in a Continuous Crystal Gamma Camera. , 2006, , .		1
79	Resolution enhancement in digital x-ray imaging. Physics in Medicine and Biology, 2006, 51, 2415-2439.	1.6	2
80	A multipinhole small animal SPECT system with submillimeter spatial resolution. Medical Physics, 2006, 33, 1259-1268.	1.6	82
81	Resolution enhancement in dual-energy x-ray imaging. , 2005, 5747, 614.		1
82	A high efficiency small animal imaging system based on position sensitive avalanche photodiodes. , 2005, , .		1
83	Evaluation of a full-scale gas microstrip detector for low-dose X-ray imaging. Nuclear Instruments and Methods in Physics Research, Section A: Accelerators, Spectrometers, Detectors and Associated Equipment, 2005, 536, 52-60.	0.7	19
84	Physical characteristics of a low-dose gas microstrip detector for orthopedic x-ray imaging. Medical Physics, 2005, 32, 1193-1204.	1.6	25
85	High Resolution Position Sensitive Avalanche Photo Diode Gamma Ray Imaging. , 0, , .		2
86	Pincushion Distortion Correction in Position Sensitive Avalanche Photodiodes. , 0, , .		3
87	Investigation of a Continuous Crystal PSAPD-Based Gamma Camera. , 0, , .		0